



## Evidence of Galaxy Cluster Motions with the Kinematic Sunyaev-Zel'dovich Effect

Nick Hand,<sup>1,2</sup> Graeme E. Addison,<sup>3</sup> Eric Aubourg,<sup>4</sup> Nick Battaglia,<sup>5</sup> Elia S. Battistelli,<sup>6</sup> Dmitry Bizyaev,<sup>7</sup>  
 J. Richard Bond,<sup>8</sup> Howard Brewington,<sup>7</sup> Jon Brinkmann,<sup>7</sup> Benjamin R. Brown,<sup>9</sup> Sudeep Das,<sup>10,11</sup> Kyle S. Dawson,<sup>12</sup>  
 Mark J. Devlin,<sup>13</sup> Joanna Dunkley,<sup>3</sup> Rolando Dunner,<sup>14</sup> Daniel J. Eisenstein,<sup>15</sup> Joseph W. Fowler,<sup>16</sup> Megan B. Gralla,<sup>17</sup>  
 Amir Hajian,<sup>8</sup> Mark Halpern,<sup>18</sup> Matt Hilton,<sup>19</sup> Adam D. Hincks,<sup>8,20</sup> Renée Hlozek,<sup>2</sup> John P. Hughes,<sup>21</sup> Leopoldo Infante,<sup>14</sup>  
 Kent D. Irwin,<sup>16</sup> Arthur Kosowsky,<sup>9,22</sup> Yen-Ting Lin,<sup>23</sup> Elena Malanushenko,<sup>7</sup> Viktor Malanushenko,<sup>7</sup>  
 Tobias A. Marriage,<sup>17</sup> Danica Marsden,<sup>24</sup> Felipe Menanteau,<sup>21</sup> Kavilan Moodley,<sup>25</sup> Michael D. Niemack,<sup>16</sup>  
 Michael R. Nolta,<sup>8</sup> Daniel Oravetz,<sup>7</sup> Lyman A. Page,<sup>20</sup> Nathalie Palanque-Delabrouille,<sup>26</sup> Kaike Pan,<sup>7</sup>  
 Erik D. Reese,<sup>13</sup> David J. Schlegel,<sup>11</sup> Donald P. Schneider,<sup>27,28</sup> Neelima Sehgal,<sup>2</sup> Alaina Shelden,<sup>7</sup>  
 Jon Sievers,<sup>20,8</sup> Cristóbal Sifón,<sup>14</sup> Audrey Simmons,<sup>7</sup> Stephanie Snedden,<sup>7</sup> David N. Spergel,<sup>2</sup>  
 Suzanne T. Staggs,<sup>20</sup> Daniel S. Swetz,<sup>16</sup> Eric R. Switzer,<sup>8</sup> Hy Trac,<sup>5</sup> Benjamin A. Weaver,<sup>29</sup>  
 Edward J. Wollack,<sup>30</sup> Christophe Yèche,<sup>26</sup> and Caroline Zunckel<sup>25</sup>

<sup>1</sup>*Department of Astronomy, University of California, Berkeley, California 94720 USA*

<sup>2</sup>*Department of Astrophysical Sciences, Princeton University, Princeton, New Jersey 08544 USA*

<sup>3</sup>*Sub-department of Astrophysics, University of Oxford, Denys Wilkinson Building, Keble Road, Oxford OX1 3RH UK*

<sup>4</sup>*APC, University of Paris Diderot, CNRS/IN2P3, CEA/IRFU, Observatoire de Paris, Sorbonne Paris Cité, France*

<sup>5</sup>*Department of Physics, Carnegie Mellon University, Pittsburgh, Pennsylvania 15213 USA*

<sup>6</sup>*Department of Physics, University of Rome "La Sapienza," Piazzale Aldo Moro 5, I-00185 Rome, Italy*

<sup>7</sup>*Apache Point Observatory, P.O. Box 59, Sunspot, New Mexico 88349 USA*

<sup>8</sup>*Canadian Institute for Theoretical Astrophysics, University of Toronto, Toronto, ON M5S 3H8 Canada*

<sup>9</sup>*Department of Physics and Astronomy, University of Pittsburgh, Pittsburgh, Pennsylvania 15260 USA*

<sup>10</sup>*Department of Physics, University of California, Berkeley California 94720 USA*

<sup>11</sup>*Lawrence Berkeley National Laboratory, 1 Cyclotron Road, Berkeley, California 94720 USA*

<sup>12</sup>*Department of Physics and Astronomy, University of Utah, Salt Lake City, Utah 84112 USA*

<sup>13</sup>*Department of Physics and Astronomy, University of Pennsylvania, Philadelphia, Pennsylvania 19104 USA*

<sup>14</sup>*Departamento de Astronomía y Astrofísica, Pontificia Universidad Católica de Chile, Santiago 22 Chile*

<sup>15</sup>*Harvard College Observatory, 60 Garden Street, MS 20, Cambridge, Massachusetts 02138 USA*

<sup>16</sup>*NIST Quantum Devices Group, 325 Broadway Mailcode 817.03, Boulder, Colorado 80305 USA*

<sup>17</sup>*Department of Physics and Astronomy, The Johns Hopkins University, Baltimore, Maryland 21218 USA*

<sup>18</sup>*Department of Physics and Astronomy, University of British Columbia, Vancouver, BC V6T 1Z4 Canada*

<sup>19</sup>*School of Physics and Astronomy, University of Nottingham, University Park, Nottingham, NG7 2RD UK*

<sup>20</sup>*Joseph Henry Laboratories of Physics, Princeton University, Princeton, New Jersey 08544 USA*

<sup>21</sup>*Department of Physics and Astronomy, Rutgers University, Piscataway, New Jersey 08854 USA*

<sup>22</sup>*Pittsburgh Particle Physics, Astrophysics, and Cosmology Center, University of Pittsburgh,  
 Pittsburgh Pennsylvania 15260, USA*

<sup>23</sup>*Institute of Astronomy and Astrophysics, Academia Sinica, Taipei, Taiwan*

<sup>24</sup>*Department of Physics, University of California, Santa Barbara, California 93106 USA*

<sup>25</sup>*Astrophysics and Cosmology Research Unit, School of Mathematical Sciences, University of KwaZulu-Natal,  
 Durban 4041, South Africa*

<sup>26</sup>*CEA, Centre de Saclay, IRFU, 91191 Gif-sur-Yvette, France*

<sup>27</sup>*Department of Astronomy and Astrophysics, The Pennsylvania State University, University Park, Pennsylvania 16802 USA*

<sup>28</sup>*Institute for Gravitation and the Cosmos, The Pennsylvania State University, University Park, Pennsylvania 16802 USA*

<sup>29</sup>*Center for Cosmology and Particle Physics, New York University, New York, New York 10003 USA*

<sup>30</sup>*Code 553/665, NASA/Goddard Space Flight Center, Greenbelt, Maryland 20771 USA*

(Received 5 March 2012; revised manuscript received 8 June 2012; published 23 July 2012)

Using high-resolution microwave sky maps made by the Atacama Cosmology Telescope, we for the first time present strong evidence for motions of galaxy clusters and groups via microwave background temperature distortions due to the kinematic Sunyaev-Zel'dovich effect. Galaxy clusters are identified by their constituent luminous galaxies observed by the Baryon Oscillation Spectroscopic Survey, part of the Sloan Digital Sky Survey III. We measure the mean pairwise momentum of clusters, with a probability of the signal being due to random errors of 0.002, and the signal is consistent with the growth of cosmic structure in the standard model of cosmology.

DOI: [10.1103/PhysRevLett.109.041101](https://doi.org/10.1103/PhysRevLett.109.041101)

PACS numbers: 98.80.Es, 98.62.Py, 98.65.Cw, 98.70.Vc

*Introduction.*—The growth of cosmic structure over the history of the Universe inevitably results not only in the formation of dense objects, but also in motions of these objects. Measurements of these motions have the potential to provide both a valuable consistency check on the standard cosmological model, and also an independent route to constraining cosmological parameters and the nature of dark energy.

In 1972, Sunyaev and Zel’dovich realized that a moving galaxy cluster, which is largely composed of hot, ionized gas in a dark matter potential well, will induce a small brightness temperature shift in the microwave radiation passing through it. The shift is proportional to both the mass in electrons and the line-of-sight velocity of the cluster with respect to the microwave background rest frame [1,2]. This kinematic Sunyaev-Zel’dovich (kSZ) effect is distinct from the thermal SZ (tSZ) effect, in which scattering from the same hot cluster gas creates a spectral distortion (see [3] for a review). In high-mass clusters ( $M \simeq 10^{15}$  solar masses), the tSZ signal is typically a factor of 20 larger than the kSZ signal; however, the two signals are comparable for the low-mass clusters ( $M \simeq 10^{13} M_{\odot}$ ) which are far more abundant. (For brevity, we refer to any object with mass larger than  $10^{13} M_{\odot}$  as a cluster, even though objects below  $10^{14} M_{\odot}$  are usually referred to as “groups.”) The tSZ effect from large clusters is now regularly observed in blind surveys [4–7], but only upper limits for the kSZ effect from individual galaxy clusters have been achieved to date [8–12].

In this Letter, we present clear statistical evidence of the motions of galaxy clusters through their kSZ signal in arcminute-resolution microwave maps made with the Atacama Cosmology Telescope (ACT) [13]. Luminous galaxies are associated with galaxy clusters [14,15], and we use the Sloan Digital Sky Survey III (SDSS-III) Baryon Oscillation Spectroscopic Survey (BOSS) [16] catalog of these galaxies as galaxy cluster proxies, giving the sky location and redshift for thousands of potential clusters. We then treat the effective microwave temperature at 148 GHz measured by ACT in the direction of the cluster as a noisy estimator of the cluster’s line-of-sight momentum, due to the kSZ temperature shift from that cluster. Individual cluster momentum measurements have a low

signal-to-noise ratio, but we combine a large number of differential measurements to obtain estimates of the mean relative momentum of cluster pairs in bins of comoving cluster separation. This statistic is insensitive to the tSZ signal, galaxy emission, and other sky signals in the ACT data. The conventional scenario of structure formation, driven by gravitational attraction, predicts that any pair of clusters should have a slight tendency to be moving towards each other rather than away from each other [17,18], and we see the expected signal in our data at a high statistical significance.

*Survey data sets.*—We make use of two astronomical survey data sets. The first is a 148 GHz sky map from ACT, a dedicated microwave survey telescope in the Atacama Desert of Chile. The map covers a strip approximately  $3^{\circ}$  wide and  $110^{\circ}$  long with an angular resolution of  $1.4'$ , centered on the celestial equator and obtained over three observing seasons from 2008 to 2010 [13]. We match-filter the ACT 148 GHz map with a characteristic filter scale at the map resolution of  $1.4'$  [19], to suppress noise from the primary microwave background fluctuations. Filtered map pixels are  $0.5'$  square, and have a noise per pixel ranging from 15 to 25  $\mu\text{K}$  brightness temperature; the map is calibrated to 2% by comparing with WMAP [20]. Imperfect knowledge of the beam profile gives an additional 1% calibration uncertainty on galaxy cluster scales. (A similar map at 218 GHz has higher noise and is used only for Table I below.)

The second data set is a catalog of luminous galaxies from BOSS Data Release 9 (a combination of the CMASS and LOWZ samples from DR9), a component of the Sloan Digital Sky Survey III [22–24]. The catalog contains 27 291 galaxies in a 220-square-degree region overlapping the ACT sky region (right ascension range  $-43^{\circ}$  to  $+45^{\circ}$ ). Galaxies are selected to lie at least  $1'$  away from any radio source in the 1.4 GHz FIRST radio catalog [25]; radio contamination is not a significant issue. Spectroscopic redshifts range from  $z = 0.05$  to  $z = 0.8$  with a mean redshift of 0.51. Luminosities are estimated as in Ref. [19], with an additional mean luminosity evolution correction as given in Ref. [26]. A halo-model correlation function analysis shows that most of the BOSS galaxies reside in haloes with

TABLE I. Mean brightness temperature fluctuations in sky directions corresponding to the BOSS DR9 galaxies, in bins of galaxy luminosity. The right column corresponds to the tSZ brightness temperature at 148 GHz,  $\delta T_{\text{tSZ}} \equiv \delta T_{148} - 0.325 \delta T_{218}$ , projecting out a dust emission component [21]. The ACT maps are match-filtered at an angular scale of  $1.4'$ , equal to the beam size at 148 GHz, then subpixelized, convolved with the beam profile, and summed over all subpixels within  $4''$  of the galaxy.

Bin	$N_{\text{gal}}$	$\langle L_{0.1r} \rangle 10^{10} L_{\odot}$	$L_{0.1r}$ Range $10^{10} L_{\odot}$	$\langle z \rangle$	$\delta T_{148} \mu\text{K}$	$\delta T_{218} \mu\text{K}$	$\delta T_{\text{tSZ}} \mu\text{K}$
1	225	23.3	17.7–73.5	0.65	$-6.98 \pm 1.69$	$+1.35 \pm 2.59$	$-7.42 \pm 1.89$
2	1326	13.1	11.0–17.7	0.61	$-1.33 \pm 0.72$	$+3.46 \pm 1.06$	$-2.45 \pm 0.80$
3	4100	9.0	7.8–11.0	0.57	$-0.11 \pm 0.38$	$+2.16 \pm 0.60$	$-0.81 \pm 0.43$
4	8467	6.6	5.7–7.8	0.51	$+0.35 \pm 0.28$	$+2.17 \pm 0.41$	$-0.36 \pm 0.31$
5	13173	4.3	0.01–5.7	0.48	$+0.43 \pm 0.22$	$+1.53 \pm 0.33$	$-0.07 \pm 0.24$
total	27291	6.3	0.01–73.5	0.51	$+0.17 \pm 0.15$	$+1.92 \pm 0.22$	$-0.45 \pm 0.17$

masses around  $10^{13}$  solar masses, with around 10% to 15% in haloes as large as  $10^{14}M_{\odot}$  [27].

To estimate the microwave temperature distortion  $T_i$  associated with galaxy  $i$ , we follow the procedure used in Ref. [19]: a  $10'$  by  $10'$  submap centered on the galaxy is repixelized into  $0.0625'$  subpixels, convolved with the ACT beam profile to smooth the map, and then averaged over all subpixels within  $1'$  of the galaxy. The  $1'$  binning radius maximizes the signal-noise ratio of our kSZ detection, but varying the binning radius between  $4''$  and  $4'$  only marginally changes the detection significance.

The most luminous galaxies in our catalog have the largest halo masses. To confirm this, we divide our sample into five luminosity bins; Table I displays the mean central temperature distortion corresponding to the galaxies in each bin. The rightmost column gives the tSZ distortion brightness temperature at 148 GHz, with the next-largest component due to dust emission projected out [21]; this is obtained from a linear combination of ACT 148 and 218 GHz signals. Galaxies in the three highest luminosity bins, corresponding to about 20% of the total, show mean temperature decrements consistent with halo-model cluster masses [27] and with the mean temperature decrements found in Ref. [19].

*Mean pairwise momentum.*—Combining the above survey data provides a set of galaxy cluster sky positions and redshifts (from the luminous galaxy positions and redshifts) and line-of-sight momenta (from the ACT temperature). To compare this data set with cosmological models, consider the mean pairwise momentum statistic:

$$p_{\text{pair}}(r) \equiv \langle (\mathbf{p}_i - \mathbf{p}_j) \cdot \hat{\mathbf{r}}_{ij} \rangle, \quad (1)$$

where galaxy cluster  $i$  has momentum  $\mathbf{p}_i$  and comoving position  $\mathbf{r}_i$ , the comoving separation vector between a pair of clusters  $i$  and  $j$  is  $\mathbf{r}_{ij} \equiv \mathbf{r}_i - \mathbf{r}_j$ , overhats denote unit vectors, and the average on the right side of the equation is over all cluster pairs in a bin around comoving separation  $r \equiv |\mathbf{r}_{ij}|$ . If two galaxy clusters are moving towards each other, their contribution to  $p_{\text{pair}}(r)$  will be negative, and if moving apart, positive. An estimator of  $p_{\text{pair}}(r)$  using only line-of-sight momenta is [28]

$$\tilde{p}_{\text{pair}}(r) = \frac{\sum_{i < j} (\mathbf{p}_i \cdot \hat{\mathbf{r}}_i - \mathbf{p}_j \cdot \hat{\mathbf{r}}_j) c_{ij}}{\sum_{i < j} c_{ij}^2}, \quad (2)$$

$$c_{ij} \equiv \hat{\mathbf{r}}_{ij} \cdot \frac{\hat{\mathbf{r}}_i + \hat{\mathbf{r}}_j}{2} = \frac{(r_i - r_j)(1 + \cos\theta)}{2\sqrt{r_i^2 + r_j^2 - 2r_i r_j \cos\theta}}, \quad (3)$$

where  $\theta$  is the angular separation between two clusters on the sky and  $r_i \equiv |\mathbf{r}_i|$  is the comoving distance to cluster  $i$ , which can be computed from the cluster redshift using standard  $\Lambda$ CDM cosmological parameters [29]. (The cluster velocity gives negligible contribution to the distance

estimate for clusters at a cosmological distance, and a bias in estimating Eq. (2) which is small compared to the measurement errors.) The statistic  $p_{\text{pair}}(r)$  is equal to the familiar mean pairwise velocity  $v_{\text{pair}}(r)$  [30–32] times the average mass of the clusters in the sample.

We can measure the line-of-sight component of the momentum via the kSZ microwave temperature fluctuation,  $T_{\text{kSZ},i} \equiv -N_{\text{kSZ}} \mathbf{p}_i \cdot \hat{\mathbf{r}}_i$ , assuming that the ratio of the total cluster mass to its mass in hot gas is simply the universal ratio of matter density  $\Omega_m$  to baryon density  $\Omega_b$  [33]. The normalization  $N_{\text{kSZ}}$  depends on the pixel scale and beam size of the microwave map, and the cluster density profile. Simulations including these effects [34] give an expected mean temperature signal in the ACT 148 GHz map of 1.6 and 0.3  $\mu\text{K}$  for clusters with a typical line-of-sight velocity of 200 km/s and masses  $10^{14}$  and  $10^{13}M_{\odot}$ .

The statistic  $p_{\text{pair}}(r)$  is both linear and differential, giving it desirable systematic error properties [35]. Any microwave temperature signal associated with individual galaxy clusters, like the tSZ effect, will average to zero as long as it does not depend on the relative distance between cluster pairs. Redshift-dependent signals can contribute to  $p_{\text{pair}}(r)$  and be confused with the cluster kSZ signal, including infrared emission from galaxies in the cluster (which increases with redshift out to  $z = 2$ ), any radio source emission, and small variations of the tSZ signal due to evolution of average cluster mass and temperature. However, we can measure these effects on average by simply finding the average microwave temperature  $\mathcal{T}(z)$  corresponding to clusters at a given redshift, and correcting the temperature in the direction of an individual galaxy cluster for this redshift-dependent piece. We evaluate a smoothed  $\mathcal{T}(z)$  by averaging the temperature towards all galaxies, each with redshift  $z_i$  and a Gaussian weight factor  $\exp[-(z - z_i)^2/2\sigma_z^2]$  with  $\sigma_z = 0.01$ ; our results are nearly insensitive to the value of  $\sigma_z$  within a wide range. The resulting  $\mathcal{T}(z)$  has a mean near zero and an absolute value of up to 3  $\mu\text{K}$ .

We thus evaluate the mean pairwise kSZ signal, correcting for possible redshift-dependent temperature contributions, as

$$\tilde{p}_{\text{kSZ}}(r) = - \frac{\sum_{i < j} [(T_i - \mathcal{T}(z_i)) - (T_j - \mathcal{T}(z_j))] c_{ij}}{\sum_{i < j} c_{ij}^2}. \quad (4)$$

This quantity differs from Eq. (2) by the amplitude factor  $N_{\text{kSZ}}$ . Figure 1 displays this statistic for the ACT pixel temperatures corresponding to the 5000 most luminous BOSS DR9 galaxies in the ACT sky region ( $L > 8.1 \times 10^{10}L_{\odot}$ ); this luminosity cut minimizes the total noise from combined Poisson and pixel noise. Also displayed is the signal extracted from a kSZ-only sky simulation, based on underlying large-volume cosmological simulations [34],

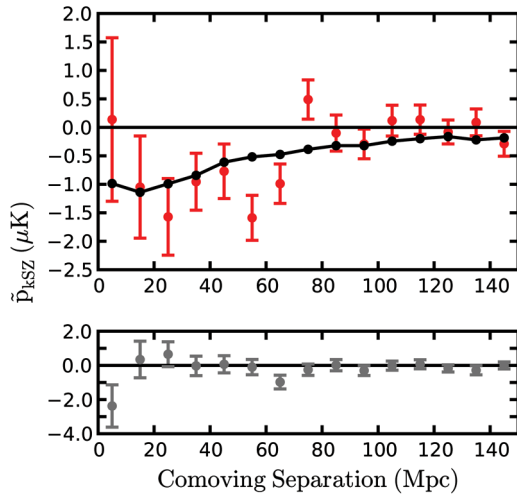


FIG. 1 (color online). The upper panel shows the mean pairwise momentum estimator, Eq. (4), for the 5000 most luminous BOSS DR9 galaxies within the ACT sky region (red points), with bootstrap errors. The solid line is derived from numerical kSZ simulations [34] using a halo mass cutoff of  $M_{200} = 4.1 \times 10^{13} M_{\odot}$ . The probability of the data given a null signal is  $2.0 \times 10^{-3}$  including bin covariances. The lower panel displays the same sum but with randomized map positions, and is consistent with a null signal.

adjusting the mass limit of the simulation halos to give the best fit to the data. We infer that our galaxy luminosity cut corresponds to a cluster halo mass limit of roughly  $M_{200} \approx 4.1 \times 10^{13} M_{\odot}$  and a mean cluster halo mass of  $M_{200} = 6.5 \times 10^{13} M_{\odot}$ . Error bars are estimated via bootstrap resampling. Neighboring bins have a mean correlation of 0.25 and we include smaller mean correlations out to a 5-bin separation, as determined using independent simulation volumes.

The measured points largely fall below zero and have  $\Delta\chi^2 = 23$  for 15 degrees of freedom, compared to the best-fit model. The model is a good fit to the data: 13% of random data realizations with the same normal errors and correlations have larger  $\Delta\chi^2$ . The measured points have  $\Delta\chi^2 = 43$  for 15 degrees of freedom, compared to a null signal; the probability of random noise having  $\Delta\chi^2$  at least this large is  $2.0 \times 10^{-3}$  including correlations. The measured points approach zero signal as the comoving pair separation increases, which demonstrates that the signal depends on spatial separation, not redshift separation.

Null tests are simple, as the statistic is essentially a sum of pixel temperatures, half with positive and half with negative signs, with weights corresponding to relative galaxy positions. Figure 1 also displays the null test corresponding to using the same weights but random pair positions compared to the signal plot ( $\Delta\chi^2 = 11.6$  for 15 degrees of freedom). Success of this null test verifies that the function  $\mathcal{T}(z)$  correctly models any redshift-dependent contributions to the microwave signal. Changing the sign in the second term of Eq. (4) from

negative to positive also gives a null signal ( $\Delta\chi^2 = 9.9$  for 15 degrees of freedom).

*Discussion and prospects.*—The signal in Fig. 1 represents the first measurement of the cosmic velocity field made directly with respect to the rest frame of the Universe. It is consistent with simulations based on the standard cosmological model. This signal is also the first clear evidence for the kinematic Sunyaev-Zel’dovich effect. A recent attempt by Kashlinsky *et al.* to measure the large-scale bulk flow via the galaxy cluster kSZ signal uses galaxy clusters from x-ray surveys and searches for an overall dipole dependence of the microwave temperature in the WMAP data at these locations [36,37]. However, Keisler [38] found the first reported detection was not statistically significant. Osborne *et al.* [39] reanalyzed the most recent results including both a monopole and dipole term, obtaining limits on a bulk flow a factor of 3 below the reported detection of Ref. [37]. Mody and Hajian [40] also fail to reproduce the bulk flow result using Planck and ROSAT galaxy clusters. Planck will soon make a more precise test of this reported large-scale flow [41]. The statistic used in this paper is differential, which mitigates many of the potential systematic errors affecting bulk flow measurements, but also is not sensitive to an overall bulk flow.

Most previous work on peculiar velocities using optical observations has measured the properties of the local bulk flow, but has not been able to extend measurements to cosmologically interesting distances. The traditional method of measuring velocities—a Doppler shift of an object’s radiation spectrum—is very challenging at cosmological distances because the spectrum of an object is redshifted due to the expansion of the Universe, and this cosmological redshift is typically large compared to the velocity frequency shift. Precise distance measurements are required, a difficult observational problem. Recent optical work [42] extends to around 100 Mpc, a redshift of  $z = 0.02$ , while this paper uses galaxy cluster velocities out to  $z = 0.8$ . Future large optical surveys such as the LSST may enable competitive cosmological velocity surveys using large catalogs of standard candles for distance measurements [43].

The evidence for a nonzero mean pairwise momentum from a kSZ signal presented here can also be interpreted as a measure of baryons on cluster length scales; a deficit of observed baryons has long been a cosmological puzzle [44]. Our signal is roughly consistent with the standard baryon fraction based on primordial nucleosynthesis, given independent halo mass estimates based on clustering of our luminous galaxy sample. This issue will be addressed in a future paper.

Future improved measurements of the mean pairwise velocity have the potential to put strong constraints on dark energy and modified gravity [45–47]. The measurement we have presented here is the first step on a new path to constraining structure growth in the Universe.

This work was supported by the U.S. National Science Foundation through Grants AST-0408698 for the ACT project, and PHY-0355328, AST-0707731 and PIRE-0507768 (Grant number OISE-0530095). The PIRE program made possible exchanges between Chile, South Africa, Spain and the U.S. that enabled this research program. N.H. was partly supported by the Berkeley Fellowship for Graduate Study. A.K. was partly supported by NSF grant AST-0807790. Funding was also provided by Princeton University and the University of Pennsylvania. ACT mapmaking computation was performed on the GPC supercomputer at the SciNet HPC Consortium; SciNet is funded by the Canada Foundation for Innovation under the auspices of Compute Canada, the Government of Ontario, Ontario Research Fund—Research Excellence, and the University of Toronto. ACT operates in the Chajnantor Science Preserve in northern Chile under the auspices of the Comisión Nacional de Investigación Científica y Tecnológica (CONICYT). This work made use of the NASA Astrophysical Data System for bibliographic information. Funding for SDSS-III has been provided by the Alfred P. Sloan Foundation, the Participating Institutions, the National Science Foundation, and the U.S. Department of Energy Office of Science. The SDSS-III web site is <http://www.sdss3.org/>. SDSS-III is managed by the Astrophysical Research Consortium for the Participating Institutions of the SDSS-III Collaboration including the University of Arizona, the Brazilian Participation Group, Brookhaven National Laboratory, University of Cambridge, Carnegie Mellon University, University of Florida, the French Participation Group, the German Participation Group, Harvard University, the Instituto de Astrofísica de Canarias, the Michigan State/Notre Dame/JINA Participation Group, Johns Hopkins University, Lawrence Berkeley National Laboratory, Max Planck Institute for Astrophysics, New Mexico State University, New York University, Ohio State University, Pennsylvania State University, University of Portsmouth, Princeton University, the Spanish Participation Group, University of Tokyo, University of Utah, Vanderbilt University, University of Virginia, University of Washington, and Yale University. We acknowledge Roman Juskiewicz for pioneering work in the field of mean pairwise velocities.

- 
- [1] R.A. Sunyaev and Ya.B. Zel'dovich, *Comments Astrophys. Space Phys.* **4**, 173 (1972).  
 [2] R.A. Sunyaev and Ya.B. Zel'dovich, *Mon. Not. R. Astron. Soc.* **190**, 413 (1980).  
 [3] J.E. Carlstrom, G.P. Holder, and E.D. Reese, *Annu. Rev. Astron. Astrophys.* **40**, 643 (2002).  
 [4] T. Marriage *et al.*, *Astrophys. J.* **737**, 61 (2011).  
 [5] R. Williamson *et al.*, *Astrophys. J.* **738**, 139 (2011).  
 [6] A.D. Hincks *et al.*, *Astrophys. J. Suppl. Ser.* **191**, 423 (2010).  
 [7] K. Vanderlinde *et al.*, *Astrophys. J.* **722**, 1180 (2010).

- [8] W.L. Holzapfel, P.A.R. Ade, S.E. Church, P.D. Mouskoff, Y. Rephaeli, T.M. Wilbanks, and A.E. Lange, *Astrophys. J.* **481**, 35 (1997).  
 [9] P.D. Mouskoff, P.A.R. Ade, S.W. Allen, S.E. Church, A.C. Edge, K.M. Ganga, W.L. Holzapfel, A.E. Lange, B.K. Rownd, B.J. Philhour, and M.C. Runyan, *Astrophys. J.* **538**, 505 (2000).  
 [10] B.A. Benson, S.E. Church, P.A.R. Ade, J.J. Bock, K.M. Ganga, J.R. Hinderks, P.D. Mouskoff, B. Philhour, M.C. Runyan, and K.L. Thompson, *Astrophys. J.* **592**, 674 (2003).  
 [11] M. Zemcov, M. Halpern, C. Borys, S. Chapman, W. Holland, E. Pierpaoli, and D. Scott, *Mon. Not. R. Astron. Soc.* **346**, 1179 (2003).  
 [12] P.D. Mouskoff, P.F. Horner, J. Aguirre, J.J. Bock, E. Egami, J. Glenn, S.R. Golwala, G. Laurent, H.T. Nguyen, and J. Sayers, *Mon. Not. R. Astron. Soc.* **421**, 224 (2012).  
 [13] D. Swetz *et al.*, *Astrophys. J. Suppl. Ser.* **194**, 41 (2011).  
 [14] D.J. Eisenstein *et al.*, *Astron. J.* **122**, 2267 (2001).  
 [15] S. Ho, Y.T. Lin, D. Spergel, and C.M. Hirata, *Astrophys. J.* **697**, 1358 (2009).  
 [16] D.J. Eisenstein *et al.*, *Astron. J.* **142**, 72 (2011).  
 [17] P.J.E. Peebles, *The Large-Scale Structure of the Universe* (Princeton University Press, Princeton, NJ, 1980), p. 266.  
 [18] A. Diaferio, R.A. Sunyaev, and A. Nusser, *Astrophys. J. Lett.* **533**, L71 (2000).  
 [19] N. Hand *et al.*, *Astrophys. J.* **736**, 39 (2011).  
 [20] A. Hajian *et al.*, *Astrophys. J.* **740**, 86 (2011).  
 [21] N.R. Hall *et al.*, *Astrophys. J.* **718**, 632 (2010).  
 [22] M. Fukugita, T. Ichikawa, J.E. Gunn, M. Doi, K. Shimasaku, and D.P. Schneider, *Astron. J.* **111**, 1748 (1996).  
 [23] J.E. Gunn *et al.*, *Astron. J.* **116**, 3040 (1998).  
 [24] J.E. Gunn *et al.*, *Astron. J.* **131**, 2332 (2006).  
 [25] R.L. White, R.H. Becker, D.J. Helfand, and M.D. Gregg, *Astrophys. J.* **475**, 479 (1997).  
 [26] M. Tegmark *et al.*, *Astrophys. J.* **606**, 702 (2004).  
 [27] M. White *et al.*, *Astrophys. J.* **728**, 126 (2011).  
 [28] P.G. Ferreira, R. Juskiewicz, H.A. Feldman, M. Davis, and A.H. Jaffe, *Astrophys. J. Lett.* **515**, L1 (1999).  
 [29] J. Dunkley *et al.*, *Astrophys. J.* **739**, 52 (2011).  
 [30] M. Davis and P.J.E. Peebles, *Astrophys. J. Suppl. Ser.* **34**, 425 (1977).  
 [31] R. Juskiewicz, P.G. Ferreira, H.A. Feldman, A.H. Jaffe, and M. Davis, *Science* **287**, 109 (2000).  
 [32] H. Feldman, R. Juskiewicz, P.G. Ferreira, M. Davis, E. Gaztanaga, J. Fry, A. Jaffe, S. Chambers, L. da Costa, M. Bernardi, R. Giovanelli, M. Haynes, and G. Wegman, *Astrophys. J. Lett.* **596**, L131 (2003).  
 [33] S. Bhattacharya, T. Di Matteo, and A. Kosowsky, *Mon. Not. R. Astron. Soc.* **389**, 34 (2008).  
 [34] N. Sehgal, P. Bode, S. Das, C. Moneagudo-Hernandez, K. Huffenberger, Y.T. Lin, J.P. Ostriker, and H. Trac, *Astrophys. J.* **709**, 920 (2010).  
 [35] S. Bhattacharya and A. Kosowsky, *J. Cosmol. Astropart. Phys.* **08** (2008) 030.  
 [36] A. Kashlinsky, F. Atrio-Barandela, D. Kocevski, and H. Ebeling, *Astrophys. J. Lett.* **686**, L49 (2008).  
 [37] A. Kashlinsky, F. Atrio-Barandela, and H. Ebeling, *Astrophys. J.* **732**, 1 (2011).  
 [38] R. Keisler, *Astrophys. J. Lett.* **707**, L42 (2009).  
 [39] S.J. Osborne, D.S.Y. Mak, S.E. Church, and E. Pierpaoli, *Astrophys. J.* **737**, 98 (2011).

- 
- [40] K. Mody and A. Hajian, *Astrophys. J.* (to be published) (2012).
- [41] D. S. Y. Mak, E. Pierpaoli, and S. J. Osborne, *Astrophys. J.* **736**, 116 (2011).
- [42] H. A. Feldman, R. Watkins, and M. J. Hudson, *Mon. Not. R. Astron. Soc.* **407**, 2328 (2010).
- [43] S. Bhattacharya, A. Kosowsky, J. A. Newman, and A. R. Zentner, *Phys. Rev. D* **83**, 043004 (2011).
- [44] J. N. Bregman, *Annu. Rev. Astron. Astrophys.* **45**, 221 (2007).
- [45] S. Bhattacharya and A. Kosowsky, *Astrophys. J. Lett.* **659**, L83 (2007).
- [46] S. Bhattacharya and A. Kosowsky, *Phys. Rev. D* **77**, 083004 (2008).
- [47] A. Kosowsky and S. Bhattacharya, *Phys. Rev. D* **80**, 062003 (2009).